Impact of genetic dynamics and single-cell heterogeneity on development of nonstandard personalized medicine strategies for cancer

Robert A. Beckman[a,b,1], Gunter S. Schemmann[c,d], and Chen-Hsiang Yeang[a,e]

[a]Simons Center for Systems Biology, School of Natural Sciences, Institute for Advanced Study, Princeton, NJ 08540; [b]Center for Evolution and Cancer, Helen Diller Family Comprehensive Cancer Center, University of California, San Francisco, CA 94158; [c]Department of Molecular Biology, Princeton University, Princeton, NJ 08544; [d]World Water and Solar Technologies, Princeton, NJ 08540; and [e]Institute of Statistical Science, Academia Sinica, Taipei 115, Taiwan

Edited by Lawrence A. Loeb, University of Washington School of Medicine, Seattle, WA, and accepted by the Editorial Board July 13, 2012 (received for review February 29, 2012)

Cancers are heterogeneous and genetically unstable. Current practice of personalized medicine tailors therapy to heterogeneity between cancers of the same organ type. However, it does not yet systematically address heterogeneity at the single-cell level within a single individual's cancer or the dynamic nature of cancer due to genetic and epigenetic change as well as transient functional changes. We have developed a mathematical model of personalized cancer therapy incorporating genetic evolutionary dynamics and single-cell heterogeneity, and have examined simulated clinical outcomes. Analyses of an illustrative case and a virtual clinical trial of over 3 million evaluable "patients" demonstrate that augmented (and sometimes counterintuitive) nonstandard personalized medicine strategies may lead to superior patient outcomes compared with the current personalized medicine approach. Current personalized medicine matches therapy to a tumor molecular profile at diagnosis and at tumor relapse or progression, generally focusing on the average, static, and current properties of the sample. Nonstandard strategies also consider minor subclones, dynamics, and predicted future tumor states. Our methods allow systematic study and evaluation of nonstandard personalized medicine strategies. These findings may, in turn, suggest global adjustments and enhancements to translational oncology research paradigms.

systems biology | evolution | treatment strategy | targeted therapy | combinations

Current practice of personalized medicine designs therapy around stable differences between individual tumors. However, preexisting heterogeneity and genetic instability suggest the need for therapeutic strategies that address intratumoral heterogeneity and dynamics.

Genetic instability has been postulated to be central to tumor evolution (1). DNA sequencing reveals vast genetic variety associated with tumors: 20,000–30,000 mutations (2), about 1,000 of which are situated within exons (3) and 50–100 of which are nonsynonymous clonal mutations (4).

Mathematical models using the focused quantitative modeling methodology (5) have demonstrated that genetic instability enhances the efficiency of carcinogenesis, a result that is robust across all plausible parameter values and model types (5–7). More efficient mechanisms of carcinogenesis should be more common in clinical tumors. Driving the enhanced efficiency is the more rapid acquisition of oncogenic mutations, and quantitative analysis has suggested that tumors with three or fewer driver mutations might not be genetically unstable, a prediction that was recently confirmed for retinoblastoma (8). These models predicted heterogeneity within individual tumors, including spatial heterogeneity (9). Moreover, in contrast to an ordered series of mutational steps (10), the models predicted convergent and divergent evolution leading to overlapping but nonidentical sets of driver mutations within the same tumor (5–7). Recently, these predictions have been confirmed in renal cell cancer, where different mutations affecting the same pathway were spatially separated within the primary, reflecting convergent evolution (11). Pancreatic and breast cancers manifest genetic differences between the primary and metastases (12–15). Relapsed pediatric acute lymphoblastic leukemia (ALL) and primary adult ALL also reveal subclonal structure and divergent evolution (16–18). Additional diversity might, in principle, be detected by single-cell genomic analysis (19). In some cases, different driver mutations lead to different functional states, such as activation states of signaling pathways, within different parts of the tumor, as was seen for the mammalian target of rapamycin (*mTOR*) gene and associated pathway in renal cell cancer (11). Thus, intratumoral phenotypic and genotypic diversity is well established.

In the current personalized medicine paradigm, targeted therapies directed at specific molecular states replace nonspecific cytotoxics. Personalized medicine has the potential to transform cancer therapy and drug development (20). Tumors are stratified based on predictive biomarkers, which define molecular states, and are then matched to corresponding treatments.

A limitation is that the tumor is often characterized by a bulk measurement of the average molecular state, which may be dominated by the primary clone, without reflecting smaller subclones. A 1-cm^3 tumor mass will contain ~10^9 cells. Current sequencing technology can detect a sequence variation present in ~1:10^4 cells (19), meaning that in a 1-cm^3 tumor mass, a single variant cell is five orders of magnitude below the detection limit. Moreover, given the spatial heterogeneity demonstrated in renal cell cancer (11), even characterization of the dominant clone from a single location may be misleading (21).

Another concern is the frequent lack of biopsiable tumor throughout the clinical course, meaning that available tumor molecular information may not be current. Noninvasive methods, such as circulating tumor cells (22), plasma DNA (23), or functional imaging (24), could provide real-time information when sufficiently mature for general application. Imaging may potentially reveal spatial heterogeneity without multiple biopsies.

Dynamic resistance to therapy has been shown for many tumor types and by a variety of genetic and nongenetic mechanisms. In non-small cell lung cancer (NSCLC) treated with erlotinib

Author contributions: R.A.B., G.S.S., and C.-H.Y. designed research; R.A.B. and C.-H.Y. performed research; R.A.B., G.S.S., and C.-H.Y. contributed new reagents/analytic tools; R.A.B., G.S.S., and C.-H.Y. analyzed data; and R.A.B., G.S.S., and C.-H.Y. wrote the paper.

Conflict of interest statement: R.A.B. is a full-time employee of Daiichi Sankyo Pharmaceutical Development and is a stockholder in the Johnson & Johnson Corp. and in Daiichi Sankyo Pharmaceutical Development.

This article is a PNAS Direct Submission. L.A.L. is a guest editor invited by the Editorial Board.

[1]To whom correspondence should be addressed. E-mail: eniac1@snip.net.

This article contains supporting information online at www.pnas.org/lookup/suppl/doi:10.1073/pnas.1203559109/-/DCSupplemental.

or gefitinib, resistance mutations occur, most commonly in the target EGF receptor (EGFR) (22, 25). Other resistance mechanisms include activation of parallel signaling pathways, such as c-Met, through amplification, which is, at times, ligand-induced (26). Importantly, when erlotinib or gefitinib resistance develops, the drug's withdrawal may trigger tumor rebound, suggesting the persistence of a sensitive subpopulation below the detection limit (27). Resistance to crizotinib, a drug targeted to a unique fusion protein involving the anaplastic lymphoma kinase in NSCLC, has been documented due to mutations in the target, amplification of the target, loss of the original translocation leading to the fusion protein, increased signaling in the EGFR pathway (including 1 EGFR activating mutation), *c-Kit* amplification, and *KRAS* mutation, sometimes with more than one resistance mechanism in the same patient (28, 29). In chronic myelogenous leukemia, most therapeutic resistance is due to mutation in the targeted BCR-ABL fusion protein, and combinations may be important to delay the emergence of multiply resistant cells (30, 31). Nongenetic resistance mechanisms occur in tumors and may be immediate because they are wired into feedback loops in signaling pathways. Recent examples include resistance to vemurafenib in colorectal cancer cells (32, 33) and to PI3-kinase inhibitors (34) via up-regulation of upstream signaling pathways. Given these dynamics, there is a need to take possible future states into account, perhaps thinking several therapeutic maneuvers ahead.

We have developed methods for systematic evaluation of nonstandard personalized medicine strategies. A strategy is a data-driven method for planning a sequence of therapies, for example, when to give combination therapy as opposed to sequential high-dose therapies or when to change therapies. Like therapies, strategies may be individualized. Nonstandard personalized medicine strategies imply adjustments in current personalized medicine, as well as suggesting novel paradigms for oncology translational research.

Building on models of cancer therapy and resistance for chemotherapy (35, 36), we have created a mathematical model of cancer therapies, incorporating single-cell heterogeneity and (epi)genetic dynamics (all known mechanisms of genetic and epigenetic change) and examined the impact of various strategic choices on patient outcomes. We present an illustrative example and a clinical trial simulation with over 3 million virtual patients. We demonstrate that when subpopulations and genetic dynamics are taken into account, personalized medicine as currently practiced can be further improved by adopting new and sometimes counterintuitive strategies, including thinking several therapeutic moves ahead. The potential magnitude and significance of this improvement are substantial.

Results

Model. We created a mathematical model to predict patient outcomes (*Methods* and *SI Methods*). The model comprises two drugs, drug-1 and drug-2, and cell types representing four phenotypic states: sensitive to both drugs (S); resistant to drug-1, sensitive to drug-2 (R_1); resistant to drug-2, sensitive to drug-1 (R_2); and resistant to both drugs ($R_{1–2}$).

Tumors contain a continuously evolving mixture of the four cell types, each with its own characteristic exponential net growth rate. Cells transition between phenotypic states at each cell generation by heritable mechanisms. Each phenotypic state may correspond to many genotypes, and the net transition rate between phenotypic states is the sum of the rates from all possible mechanisms of genetic change affecting the sensitivity/resistance phenotype. Transient functional states, such as activation of signaling pathways, may be directly linked to genetic states, as recently demonstrated in renal cell cancer (11).

Assumptions include a dose-proportional decrease in the exponential growth constant with therapy. The total dose of both drugs in combination cannot exceed the normalized full dose of either drug, due to toxicity. The terms "drug-1" and "drug-2" may also refer to combinations directed at single states. For example, when there is hard-wired nongenetic resistance based on feedback activation of receptor tyrosine kinases (RTKs), such as occurs for vemurafenib and for PI3-kinase inhibitors (32–34), a combination that includes an inhibitor of the upstream RTK may be optimal for dealing with the underlying state. This optimized combination might be referred to as drug-1 because the core model deals only with genetic and epigenetic mechanisms of sensitivity and resistance (*SI Methods*).

The model outputs the number of cells of each type as a function of time and treatment. Patients begin with a minimally detectable 1-cm^3 lesion of 10^9 cells or a 5-cm^3 lesion and no $R_{1–2}$ cells. "Complete response" denotes a decrease in cells below 10^9. "Tumor progression" implies relapse and/or a doubling in cell number for detectable disease. "Relapse" denotes a return to $\geq 10^9$ cells. "Incurable" refers to any state containing $R_{1–2}$ cells. "Mortality" corresponds to a tumor burden of $\geq 10^{13}$ cells.

Illustrative Example. Fig. 1*A* illustrates how the model works for the current personalized medicine strategy. The patient presents with a single lesion of 10^9 S cells, as judged by next-generation sequencing, with sensitivity for variants of $1{:}10^4$ cells. Drug-1 is the best drug for S cells, causing a log kill within 23 d, whereas drug-2 slows S-cell growth by 90%. However, the case is constructed with undetected preexisting heterogeneity and dynamic asymmetry. Specifically, there are 10^4 preexisting R_1 cells, or 1 in 10^5, 10-fold below the level of detection. Second, transitions to drug-2 resistance occur at a rate of 4×10^{-7}, whereas acquisition of drug-1 resistance occurs 100 times more slowly (dynamic asymmetry). These assumptions are plausible for human cancers (37). In order for R_1 cells to outnumber R_2 cells, even though resistance to drug-2 occurs more quickly, a specific evolutionary history is required in which a recent event enhanced the ability to acquire drug-2 resistance. For example, if drug-2 resistance requires genetic change in both copies of a gene, change in one copy may have occurred, leading to the opportunity for rapid acquisition of drug-2 resistance through loss of heterozygosity.

In the current personalized medicine strategy (Fig. 1*A*), the patient is treated with drug-1, the best drug for S cells, based on the biopsy result and enjoys an initial complete response. However, 14 mo after initial diagnosis, relapse occurs and biopsy indicates pure R_1 cells (10^4 $R_{1–2}$ cells, resulting from random, passive acquisition of drug-2 resistance by the expanding R_1 clone, are undetected). Treatment with drug-2 ensues, resulting in another complete response. Twenty-eight months from initial diagnosis, the patient has an incurable relapse, predominantly with $R_{1–2}$ cells. The multiple relapses featured in this clinical course are typical in practice.

In contrast, in one possible nonstandard personalized medicine strategy (Fig. 1*B*), the physician considers the possible risk of undetected R_1 cells, and their ability to evolve rapidly into incurable $R_{1–2}$ cells. The physician may be considering genetic information about the likelihood of certain subclones available from the literature, such as the recent report of subclone frequencies in over 100 cases of triple-negative breast cancer (38). Accordingly, the patient is treated for 4 mo with the inferior drug for S cells, drug-2, allowing the tumor to grow slowly under careful observation but killing some of the R_1 cells if present. Subsequent switching to a 50:50 mix of the two drugs results in a complete response and an apparent cure.

By allowing the tumor to grow slowly rather than treating it with the better drug for the observed population, and by prioritizing rapid treatment of a hypothetical risk over optimally treating what is observed, the nonstandard personalized medicine approach has yielded a substantially improved outcome. Importantly, an upfront combination of the drugs might not have been sufficiently effective in preventing the emergence of the $R_{1–2}$ state.

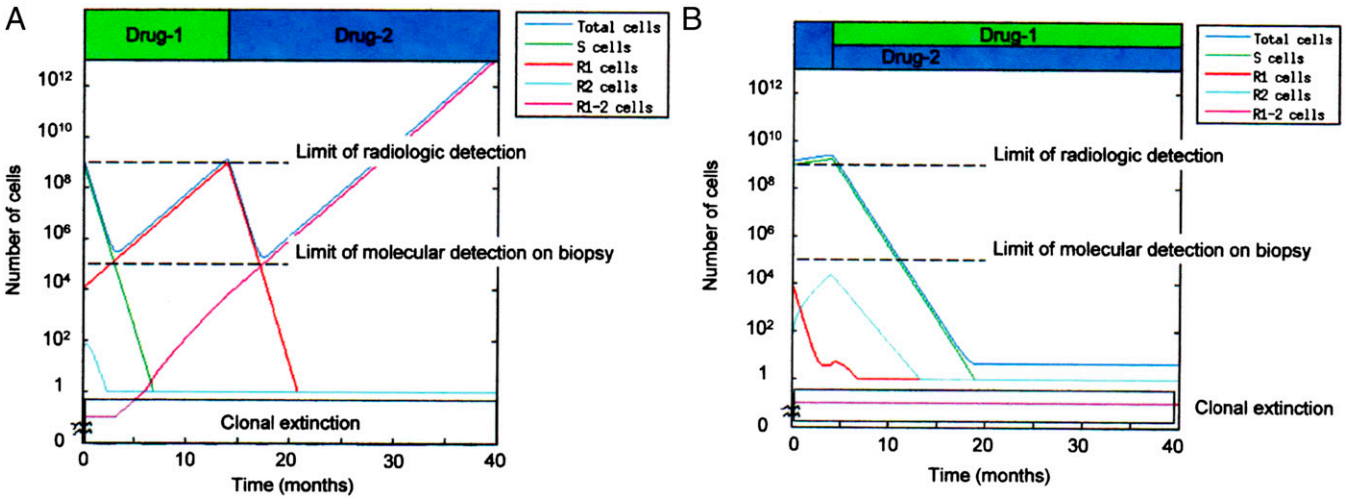

Fig. 1. Illustrative example contrasting current practice of personalized medicine (*A*) and nonstandard personalized medicine (*B*). Time (months) is on the *x* axis, and cell number is on the *y* axis. The total number of cells (*N*) is shown in blue (multiplied by 1.5 to create separation from the predominant population for clarity), S cells are shown in green, R_1 cells are shown in red, R_2 cells are shown in light blue, and R_{1-2} cells are shown in magenta. Treatments are indicated by the solid bars at the top: green is drug-1, blue is drug-2, and both colors indicate a combination. In the current personalized medicine strategy (*A*), the patient is treated with drug-1 and experiences a complete response, only to relapse 14 mo after diagnosis with R_1 cells. He/she is then treated with drug-2, experiencing a second complete response before he/she relapses with incurable R_{1-2} cells 28 mo after initial diagnosis. In the nonstandard personalized medicine strategy (*B*), the patient is treated with drug-2 for 4 mo to suppress a possible R_1 subpopulation even though it has not been detected. The bulk tumor slowly grows under observation. At 4 mo, treatment continues with an equal mixture of drug-1 and drug-2, resulting first in a complete response and then in an apparent cure. Note that initial treatment with an equal drug mixture would have been less effective in immediate eradication of R_1 cells, allowing more time for incurable R_{1-2} cells to evolve. Parameter values are provided in *SI Methods*.

Evolutionary dynamics and initial conditions affect the results. Thus, if the patient had an undetected subpopulation of R_2 cells rather than R_1 cells, the two sequences described above both lead to cure, the nonstandard sequence more rapidly (*SI Results* and Figs. S1 and S2).

A demonstration program for individual case analysis is provided on the Web (*SI Methods*).

Large-Scale Simulation. In the large-scale simulation (*Methods* and *SI Methods*), over 30 million parameter configurations are analyzed to assess the generality of the illustrative example, the potential benefits of nonstandard personalized medicine strategies, and the conditions under which minimizing the chance of transitions to incurability are an overriding strategic concern.

Parameters that were varied include proportions of different cell types, net growth rates, drug sensitivities, and transition rates between phenotypic states. Parameter ranges are derived from clinical, in vitro, and in vivo data sources, such as a series of 228 patients with pancreatic cancer with autopsies for 101 of them (39), and bracket all possible values to ensure inclusion of all possible biologically relevant scenarios. Within each parameter range, there are a large number of possible discrete values (e.g., many degrees of sensitivity/resistance are explored), and the simulation steps through every possible parameter combination once. Due to the inclusion of extreme parameter values, the parameter combinations were then prescreened, and the following were eliminated: (*i*) any combination in which one of the two drugs was not minimally effective against any cell type, because there are no strategic choices in this case, and (*ii*) any combination in which all treatment strategies resulted in survival greater than 4 y, corresponding to very slow growth rates or highly sensitive cells. Because the simulation was truncated at 5 y, it could not compare strategies in scenarios in which survival approached or exceeded this length of time (*SI Methods*).

Drug-1 is the better treatment against S cells. Survival is checked weekly, and treatments are adjusted every 45 d based on the various strategies. Ability to measure the cell populations is assumed. The simulation runs nearly 5 y (255 wk for economical data storage).

Six strategies are compared: current personalized medicine (strategy 0) and five alternatives (Table 1 and *SI Methods*). As in typical randomized oncology phase 3 trials, one strategy is "significantly better" than another if the superior strategy gives at least 8 wk of absolute improvement and 25% relative improvement in survival compared with the reference strategy. Strategy matters if at least one strategy is significantly better than another.

The resulting "clinical trial" contained 3,091,175 virtual patients, and strategy mattered for 1,001,868, showing a possible benefit of strategic choices. For the other 2 million patients, the current personalized medicine strategy gave results comparable to the other strategies. Moreover, the mean and median survival rates and percentage of 5-y survival rates seen for the simulated current personalized medicine strategy were similar to typical results for patients with metastatic solid tumors, confirming the ability of the simulation to give realistic results. Sampling of parameter values in the simulation may or may not reflect their unknown distribution in patients.

The current personalized medicine strategy was generally inferior. Other strategies produced double the mean and median survival rates (Table 2). The Kaplan–Meier survival plot over evaluable virtual patients (Fig. 2) shows a dramatic benefit of nonstandard strategies over current personalized medicine. Five-year survivorship is 0.7% for current personalized medicine and 17–20% for the other strategies (Table 2). Strategy 2.2, similar to the illustrative example, is most frequently significantly superior to the other strategies (Table 2). No strategy is inferior to the current personalized medicine strategy as frequently as it is superior, nor is the current personalized medicine strategy ever the best (Table 2).

We examined what features are required for strategy to matter (*SI Results*). Either preexisting heterogeneity or rapid genetic dynamics are generally required for strategy to matter. Given no R_1 preexisting (with drug-1 as the better drug for S, only R_1 creates strategic dilemmas), and low $S \rightarrow R_1$ transition rates,

Table 1. Treatment strategies

Strategy	Summary	Details
0	Current personalized medicine paradigm	The patient is treated with the best drug for the observed predominant cell type and switched to the alternative drug on tumor progression or relapse
1	Minimize total cell population (i.e., give the drug combination that the model predicts will do so)	Minimized at next 45-day time point
2.1	Minimize the chance of developing incurable R_{1-2} cells unless there is radiologically detectable disease burden above a "threshold" cell number; then, minimize total population	Threshold cell number to be considered radiologically detectable is 10^9 or more; minimization applies to next 45-day time point
2.2	Minimize the chance of developing incurable R_{1-2} cells unless there is a large disease burden above a threshold cell number; then, minimize total population	Threshold cell number to be considered large disease burden is 10^{11} or more; minimization applies to next 45-day time point
3	Minimize the total population unless there is an immediate threat of developing an incurable R_{1-2} cell; then, minimize R_{1-2} cells	Immediate threat is defined as predicted number of R_{1-2} cells ≥ 1 at next 45-day time point
4	Treat the most proximal threat	Estimated time to mortality from each cell type is compared with estimated time to the first incurable R_{1-2} cell; the threat estimated to have the shortest time is prioritized in treatment; mortality is defined as a tumor cell burden of 10^{13}

A strategy is a data-driven method for planning a sequence of therapies, based on both individual patient data and general oncology knowledge. The strategies discussed in this paper are examples only and are not meant to be a comprehensive list.

strategy mattered in 1.1% of evaluable cases, compared with 32.4% of evaluable cases in the overall simulation. However, we do not need both preexisting heterogeneity and rapid genetic dynamics for strategy to matter: the number of cases where it matters is relatively constant as either of these parameters alone is varied. Finally, asymmetry of transition rates, sensitivity patterns, or preexisting subpopulations are not required, not occurring more often than expected in cases where strategy matters. These results suggest that the illustrative example represents only one of many scenarios where strategy matters.

Strategy 1 differs from strategies 2–4 in that it never prioritizes prevention of R_{1-2} cell formation; instead, it simply minimizes the predicted total population. In most cases, the full benefit can be captured with this simple approach alone. By estimating the time to either incurability (τ_{1-2}) or death due to other populations, one can determine if τ_{1-2} is the shorter, indicating that the threat of incurability is more imminent than the threat of mortality from all other subpopulations (*SI Methods*). Strategy 1 is more likely to be inferior to strategies 2–4 if this condition is met (Table S1).

Discussion

We have shown that genetic dynamics and single-cell heterogeneity can have a significant impact on optimal personalized medicine strategies and that striking therapeutic gains are possible. The magnitude of the average benefit would have been significant even if applicable only to a single class of therapies and a restricted subset of patients. In contrast, a comprehensive exploration of oncology parameter space via simulation indicates that the benefit is applicable across a very broad range of therapy and tumor characteristics. We believe the systematic study of nonstandard personalized medicine strategies is an important area for experimental and theoretical investigation.

The current study is a proof of concept using a simple, focused model and is not intended to represent all known complexities of tumor behavior at either the single-cell level or the population level, where complex ecologies may provide further selection for heterogeneity. With appropriate sensitivity analyses, simple models can answer high-level focused questions ("Is the current strategy for personalized therapy of cancer the best possible?") in a way that is clear and valid across a broad range of cases (5). In this paper, we have asked this high-level focused question and tested its generality over millions of possible scenarios, with comprehensive parameter ranges based on clinical and experimental data. The high-level conclusions are shown to be robust. However, detailed conclusions will vary, depending on more detailed tumor behavior, and the model must be customized for each tumor type under consideration based on molecular and empirical knowledge. In *SI Methods*, we discuss a framework for linking the simple core strategy model presented here to molecular and

Table 2. Comparison of treatment strategy results

Strategy	0	1	2.1	2.2	3	4
Median survival*,wk	26	58	58	58	58	51
Mean survival*, wk	48.4	95.3	95.7	96.5	96.8	91.7
Survival at 5 y, %	0.7	18.7	19.0	19.7	19.4	17.6
No. of cases strategy numerically better than all others	1,538	244	4,292	60,599	2,124	2,206
No. of cases strategy significantly† better than all others	0	0	24	2,367	157	315
No. of cases significantly† better than strategy 0	N.A.	951,165	947,634	947,568	971,111	823,939
No. of cases significantly† worse than strategy 0	N.A.	6,808	5,725	2,762	630	27,597

Strategy results are based on performance in a virtual clinical trial of over 3 million evaluable cases. Evaluable means that both drugs met minimal criteria for efficacy, providing strategic choices, and that the minimum survival of the worst strategy is ≤80% of the simulation length, allowing room for other strategies to demonstrate superiority. Strategies are defined in Table 1. N.A., not applicable.
*Simulation truncated at 255 wk, which is nearly 5 y, and data can be stored as 8 bits.
†Significantly better means at least 8 wk of absolute improvement and 25% relative improvement compared with the reference strategy, in analogy to the typical minimum improvement deemed clinically significant in randomized phase 3 trials in cancer.

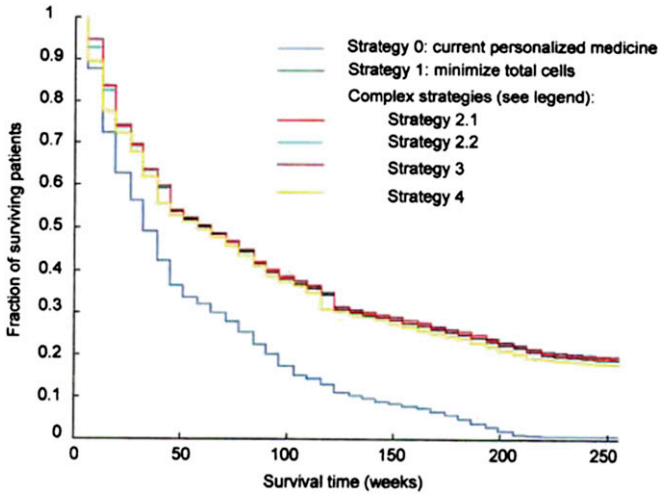

Fig. 2. Kaplan–Meier survival curves of a virtual clinical trial incorporating different strategies. Approximately 3 million evaluable virtual patients were treated with each of the strategies. The *x* axis shows time (weeks), and the *y* axis shows the surviving patient fraction. Strategy 0 (dark blue) is the current personalized medicine strategy: treatment with the best drug for the observed predominant cell type and switching to the alternative drug on tumor progression or relapse. Strategy 1 (green) minimizes total cell numbers at the next time point. Strategy 2.1 (red) minimizes the chance of developing incurable R_{1-2} cells at the next time point unless the patient has detectable disease (10^9 cells); at that point, total cell number is minimized. Strategy 2.2 (light blue) minimizes the chance of developing incurable R_{1-2} cells at the next time point unless the patient has a high disease burden (10^{11} cells); at that point, the total number of cells is minimized. Strategy 3 (magenta) minimizes the total cells at the next time point unless the predicted R_{1-2} cell population at that time point is ≥1; in that case, the R_{1-2} cell population is minimized. Strategy 4 (olive) predicts the time to mortality from each cell population and the time to "incurability" from forming R_{1-2} cells, prioritizing treatment of the most imminent threat at the next time point.

empirical knowledge of specific tumors and therapies, including complications not represented in the core model.

States in the core model correspond to heritable drug sensitivity/resistance phenotypes over all available drugs, and there may be a very large number of underlying molecular states that contribute to a single phenotype. The condensation from a large number of molecular/genetic states to a smaller number of clusters of phenotypic sensitivity/resistance profiles is essential to allow computationally feasible examination of highly innovative strategies, especially when real systems with more than two therapies are considered. Intermediate sensitivity states that may arise from haploinsufficiency or gene dosage effects must also be considered in a full model.

Similarly, the transition rate from phenotype A to phenotype B is actually the sum of individual rates from all known genetic and epigenetic mechanisms of transition at all relevant loci. Recent work on mechanisms of resistance to crizotinib (28, 29) gives an example of how multiple mechanisms can contribute to the resistance phenotype, and these processes would all have to be identified, and rates summed, to give a net transition rate. Nongenetic resistance mechanisms are addressed separately (*SI Methods*).

Relevant data sources for condensing molecular states into shared sensitivity phenotypes, or for summing transition rates to get a net transition rate, include molecularly annotated cell line panels (40), genetic data at the subclonal level from large cohorts of patients (38), computational integration of data from multiple sources along curated signaling pathways (41), and high-throughput functional genomic screens using siRNA and shRNA (42).

This illustrates the principle of linked models, some relatively simple, feeding each other information to represent a complex system. The information about the tumor type and therapies of interest can be calculated once and used to inform the focused core model through its impact on the probability distributions of parameter values. In a separate step, the core model would calculate the patient outcome resulting from a series of innovative treatment strategies.

In a comprehensive model, some information will be uncertain or missing. Therefore, advanced techniques for optimizing strategies in the face of uncertainty will be required (43). It is unknown how much missing information can be tolerated without affecting the utility of the models. This is an important area for future research. The models are a supplement to, rather than a substitute for, sound clinical judgement.

Because the number of phenotypic states is much smaller than the number of molecular states, a strategic model for cancer therapy could also become an organizing principle for our ever-expanding body of molecular data and understanding. Areas needed for progress in the treatment strategy model may correspond to key research and drug discovery priorities.

We have introduced methodology for systematic study of nonstandard personalized medicine strategies. There are key differences from the current personalized medicine paradigm. Instead of focusing on majority populations at diagnosis or at the treatment time, nonstandard personalized medicine strategies consider all subpopulations and the whole time course of possible states. In particular, nonstandard personalized medicine strategies may emphasize preventing fully resistant or incurable states by attacking their immediate precursors (*SI Methods*, Fig. S3, and Table S2). This leads to the possibility that, assuming sufficient knowledge, one might not treat initially with the targeted agent that is most effective against the predominant observed population. Although we may not have sufficient knowledge to adopt such a counterintuitive strategy at the moment, our molecular knowledge of cancer, its therapy, and its evolution is increasing rapidly. In the future, initial treatment might consider the probability distribution of current states below the detection limit and even future states. We note that current combination chemotherapy already incorporates some of these principles, although nonstandard personalized medicine may not always recommend combinations.

To facilitate application of nonstandard personalized medicine strategies, current efforts in translational oncology should be augmented in specific ways. This, in turn, may provide new directions for these fields.

Currently, biological samples exist predominantly from diagnosis and less frequently from relapse. In contrast, we suggest working backward from the fatal end states. This would require advance directives from healthy individuals to donate tumor tissue immediately on death due to cancer in much the same way that we all specify, when healthy, that we will donate organs, when feasible, after accidental death. Cell lines, patient sample banks, and patient-derived xenografts should be established from these sources, ideally paired with diagnostic samples and treatment course information.

Experimental validation of this approach could involve an in vitro or in vivo system determined by sensitivity and resistance to two drugs, with known underlying heritable molecular types. Predictable and sufficient transition rates are required. Cell populations and survival rates need to be determined under different strategic paradigms with varying initial subpopulations.

Application of nonstandard personalized medicine to cancer requires experimental validation, detailed integration of current knowledge into customized models, and further conceptual and technological advances. However, we have shown that the benefit of such an approach, when successfully applied, will be highly significant.

Methods

Model. Denote a four-component vector, $\vec{x}=(x_S, x_{R1}, x_{R2}, x_{R1-2})$, as the cell population of each class. We assume that cell death rates are zero in the absence of therapy, that all cells have the same growth rate, and that the drugs work by increasing cell death. For each class, $i \in \{S, R_1, R_2, R_{1-2}\}$, the net growth rate is $g_0 x_i + \sum_{j \neq i} T(i,j) g_0 x_j - (S_a(i,1)d_1 + S_a(i,2)d_2)x_i$. The first term corresponds to the growth rate of cell type i with a rate g_0 shared by all cell types. The second term corresponds to the transitions from all other cell types, where $T(i,j)$ specifies the transition rate (per cell per generation) from cell type j to i. We assume that (*i*) transition rates from resistant to sensitive cell types are negligible, (*ii*) the transition rate of acquiring the resistance to one drug is independent of the resistance phenotype to another drug, and (*iii*) transition rates of acquiring double resistance in one step are negligible. Thus, $T(R_1,S)=T(R_{1-2},R_2)$, $T(R_2,S)=T(R_{1-2},R_1)$, and all other entries of T are zero. The third term corresponds to the treatment-caused cell death, where $(d_1,d_2)^T \equiv \vec{d}$ represents the normalized dosages of the two drugs (d_1 is drug-1 and d_2 is drug-2) with the constraints $0 \le d_1, d_2, d_1+d_2 \le 1$ and $S_a(i,1), S_a(i,2)$ represents the sensitivities of cell type i to drug-1 and drug-2. The population dynamics of the four cell types can be compactly expressed as a matrix differential equation:

$$\frac{d\vec{x}}{dt} = \left[(I+T)g_0 - diag\left(S_a\vec{d}\right)\right] U(\vec{x}-1)\vec{x}, \qquad [1]$$

where I denotes a four-by-four identity matrix and $diag(.)$ denotes an operator of placing vector components on the diagonal entries of a zero matrix. $U(\vec{x}-1)\vec{x}$ sets component values to 0 if they are less than 1; that is, $U(\vec{x}-1)=0$ for $x<1$ and $U(\vec{x}-1)=1$ for $x \ge 1$. This term stipulates that fractional cell numbers (less than 1 cell) do not contribute to cell division.

This equation was implemented in MATLAB 7.7.0 (R2008b; MathWorks) and manually explored on a Gateway T-6836 computer with the Windows Vista (Microsoft Corporation) operating system and a 2.0-GHz Intel Core 2 Duo CPU T5750 processor to produce the illustrative example.

Large-Scale Simulation. A large-scale simulation was carried out to compare a current personalized medicine strategy with five alternative strategies for over 30 million configurations of nine parameters involving initial populations of each cell type, growth rates, drug sensitivities, and transition rates. Detailed definitions of the strategies and the parameters, as well as ranges and values of the parameters, are provided in *SI Methods*.

We can solve Eq. **1** analytically given a time-varying dosage $\vec{d}(t)$ and the initial population $\vec{x}(0)$. Insert "break points" in the time interval whenever $\vec{d}(t)$ changes or a component in $\vec{x}(t)$ crosses 1 (increases from a fractional number to a number larger than 1 or vice versa). Between any two consecutive break points, the term on the right-hand side of Eq. **1**, $[(I+T)g_0 - diag(S_a\vec{d})]U(\vec{x}-1) \equiv A$, is a constant matrix. The solution of a first-order linear matrix differential equation $\frac{d\vec{x}(t)}{dt} = A\vec{x}(t)$ is $\vec{x}(t)=e^{At}\vec{x}(0)$. Hence, $\vec{x}(t)$ can be obtained by solving the first-order linear matrix differential equation piecewise.

We implemented the simulation in a C program and ran it on 23 Hewlett Packard DL360 G7 servers in parallel. Each server contains dual Intel(R) Xeon (R) CPUs E5520 with 2.27GHz and 24 GB of main memory. The running time was approximately 1 day.

ACKNOWLEDGMENTS. We thank Arnold Levine, Director of the Simons Center for Systems Biology, Institute for Advanced Study, and Peter Goddard, Director of the Institute for Advanced Study, for hosting R.A.B. and C.H.Y. at the inception of this work. We thank Ming-Ren Yen for assistance with the large-scale simulation and Robert Shin-sheng Yuan and Cin-di Wang for Web site programming and design. We also thank Prashanth Ak, Alessandra Cesano, Robert Corringham, Lawrence Loeb, Eric Maskin, Frank McCormick, Paul Meltzer, Daniel Notterman, David Parkinson, Daniel Rabin, Guna Rajagopal, Hatem Sabaawy, Richard Simon, Alexei Vazquez, Daniel von Hoff, and Susan J. Ward for helpful discussions.

1. Loeb LA, Springgate CF, Battula N (1974) Errors in DNA replication as a basis of malignant changes. *Cancer Res* 34:2311–2321.
2. Pleasance ED, et al. (2010) A comprehensive catalogue of somatic mutations from a human cancer genome. *Nature* 463:191–196.
3. Wood LD, et al. (2007) The genomic landscapes of human breast and colorectal cancers. *Science* 318:1108–1113.
4. Parsons DW, et al. (2008) An integrated genomic analysis of human glioblastoma multiforme. *Science* 321:1807–1812.
5. Beckman RA (2010) Efficiency of carcinogenesis: Is the mutator phenotype inevitable? *Semin Cancer Biol* 20:340–352.
6. Beckman RA, Loeb LA (2006) Efficiency of carcinogenesis with and without a mutator mutation. *Proc Natl Acad Sci USA* 103:14140–14145.
7. Beckman RA (2009) Mutator mutations enhance tumorigenic efficiency across fitness landscapes. *PLoS ONE* 4:e5860.
8. Zhang J, et al. (2012) A novel retinoblastoma therapy from genomic and epigenetic analyses. *Nature* 481:329–334.
9. Loeb LA, Bielas JH, Beckman RA (2008) Cancers exhibit a mutator phenotype: Clinical implications. *Cancer Res* 68:3551–3557, discussion 3557.
10. Fearon ER, Vogelstein B (1990) A genetic model for colorectal tumorigenesis. *Cell* 61: 759–767.
11. Gerlinger M, et al. (2012) Intratumor heterogeneity and branched evolution revealed by multiregion sequencing. *N Engl J Med* 366:883–892.
12. Yachida S, et al. (2010) Distant metastasis occurs late during the genetic evolution of pancreatic cancer. *Nature* 467:1114–1117.
13. Klein CA, Hölzel D (2006) Systemic cancer progression and tumor dormancy: Mathematical models meet single cell genomics. *Cell Cycle* 5:1788–1798.
14. Fujii H, Marsh C, Cairns P, Sidransky D, Gabrielson E (1996) Genetic divergence in the clonal evolution of breast cancer. *Cancer Res* 56:1493–1497.
15. Shah SP, et al. (2009) Mutational evolution in a lobular breast tumour profiled at single nucleotide resolution. *Nature* 461:809–813.
16. Mullighan CG, et al. (2008) Genomic analysis of the clonal origins of relapsed acute lymphoblastic leukemia. *Science* 322:1377–1380.
17. Anderson K, et al. (2011) Genetic variegation of clonal architecture and propagating cells in leukaemia. *Nature* 469:356–361.
18. Notta F, et al. (2011) Evolution of human BCR-ABL1 lymphoblastic leukaemia-initiating cells. *Nature* 469:362–367.
19. Fox EJ, Salk JJ, Loeb LA (2009) Cancer genome sequencing—An interim analysis. *Cancer Res* 69:4948–4950.
20. Beckman RA, Clark J, Chen C (2011) Integrating predictive biomarkers and classifiers into oncology clinical development programmes. *Nat Rev Drug Discov* 10:735–748.
21. Longo DL (2012) Tumor heterogeneity and personalized medicine. *N Engl J Med* 366: 956–957.
22. Maheswaran S, et al. (2008) Detection of mutations in EGFR in circulating lung-cancer cells. *N Engl J Med* 359:366–377.
23. Wang S, et al. (2010) Potential clinical significance of a plasma-based KRAS mutation analysis in patients with advanced non-small cell lung cancer. *Clin Cancer Res* 16: 1324–1330.
24. Orlova A, et al. (2007) Synthetic affibody molecules: A novel class of affinity ligands for molecular imaging of HER2-expressing malignant tumors. *Cancer Res* 67:2178–2186.
25. Kobayashi S, et al. (2005) *EGFR* mutation and resistance of non-small-cell lung cancer to gefitinib. *N Engl J Med* 352:786–792.
26. Turke AB, et al. (2010) Preexistence and clonal selection of MET amplification in EGFR mutant NSCLC. *Cancer Cell* 17(1):77–88.
27. Riely GJ, et al. (2007) Prospective assessment of discontinuation and reinitiation of erlotinib or gefitinib in patients with acquired resistance to erlotinib or gefitinib followed by the addition of everolimus. *Clin Cancer Res* 13:5150–5155.
28. Lovly CM, Pao W (2012) Escaping ALK inhibition: Mechanisms of and strategies to overcome resistance. *Sci Transl Med* 4:120ps2.
29. Katayama R, et al. (2012) Mechanisms of acquired crizotinib resistance in ALK-rearranged lung cancers. *Sci Transl Med* 4:120ra17.
30. Bradeen HA, et al. (2006) Comparison of imatinib mesylate, dasatinib (BMS-354825), and nilotinib (AMN107) in an *N*-ethyl-*N*-nitrosourea (ENU)-based mutagenesis screen: High efficacy of drug combinations. *Blood* 108:2332–2338.
31. Shah NP, et al. (2007) Sequential ABL kinase inhibitor therapy selects for compound drug-resistant BCR-ABL mutations with altered oncogenic potency. *J Clin Invest* 117: 2562–2569.
32. Prahallad A, et al. (2012) Unresponsiveness of colon cancer to BRAF(V600E) inhibition through feedback activation of EGFR. *Nature* 483:100–103.
33. Solit DB, Jänne PA (2012) Translational medicine: Primed for resistance. *Nature* 483: 44–45.
34. Chandarlapaty S, et al. (2011) AKT inhibition relieves feedback suppression of receptor tyrosine kinase expression and activity. *Cancer Cell* 19(1):58–71.
35. Goldie JH, Coldman AJ (1979) A mathematic model for relating the drug sensitivity of tumors to their spontaneous mutation rate. *Cancer Treat Rep* 63:1727–1733.
36. Norton L, Simon R (1976) Tumor size, sensitivity to therapy and the design of treatment protocols. *Cancer Treat Rep* 61:1307–1317.
37. Beckman RA, Loeb LA (2005) Negative clonal selection in tumor evolution. *Genetics* 171:2123–2131.
38. Shah SP, et al. (2012) The clonal and mutational evolution spectrum of primary triple-negative breast cancers. *Nature* 486:395–399.
39. Haeno H, et al. (2012) Computational modeling of pancreatic cancer reveals kinetics of metastasis suggesting optimum treatment strategies. *Cell* 148:362–375.
40. Barretina J, et al. (2012) The Cancer Cell Line Encyclopedia enables predictive modelling of anticancer drug sensitivity. *Nature* 483:603–607.
41. Heiser LM, et al. (2012) Subtype and pathway specific responses to anticancer compounds in breast cancer. *Proc Natl Acad Sci USA* 109:2724–2729.
42. Jiang H, Pritchard JR, Williams RT, Lauffenburger DA, Hemann MT (2011) A mammalian functional-genetic approach to characterizing cancer therapeutics. *Nat Chem Biol* 7(2):92–100.
43. Dutta PK (2005) *Strategies and Games: Theory and Practice* (MIT Press, Cambridge, MA).